Single- and double-photoionization cross sections of carbon dioxide (CO_2) and ionic fragmentation of CO_2^+ and CO_2^{2+}

Toshio Masuoka
Department of Applied Physics, Faculty of Engineering, Osaka City University, Sugimoto 3, Sumiyoshi-ku, Osaka 558, Japan
(Received 26 May 1994)

Single- and double-photoionization processes of carbon dioxide (CO_2) have been studied in the photon-energy region of 30–100 eV by use of time-of-flight mass spectrometry and the photoion-photoion coincidence method together with synchrotron radiation. The single- and double-photoionization cross sections of CO_2 are determined. Ion branching ratios and the partial cross sections for the individual ions, respectively produced from the precursors CO_2^+ and CO_2^{2+}, are determined separately at excitation energies where the molecular and dissociative single- and double-photoionization processes occur simultaneously. The threshold for the molecular double photoionization was found to be 37.6±0.3 eV. The thresholds for the $CO^+ + O^+$ and $C^+ + O^+$ channels of CO_2^{2+} are at 39.2±0.3 and 47.2±0.5 eV, respectively. Furthermore, in single photoionization, the production of CO_2^+ is dominant, whereas with double photoionization, dissociation becomes dominant.

PACS number(s): 33.80.Eh, 33.80.Gj

I. INTRODUCTION

The probability of two-electron ejection is important to understand electron correlations, and an accurate determination of the partial cross section for double ionization should be extended to molecules. However, since molecular double ionization is usually followed by the production of an ion pair ($A^+ + B^+$, dissociative double ionization) when excitation energy exceeds the double-photoionization threshold by a few eV, both molecular and dissociative double ionization are, in general, not accurately estimated in the determination of the double-photoionization cross section. To address this problem, the present study focuses on the determination of the partial cross sections for the single and double photoionization of carbon dioxide at excitation energies where molecular and dissociative single and double photoionization take place concomitantly.

In the present study, the time-of-flight (TOF) mass spectrometry and photoion-photoion coincidence (PIPICO) methods were used together with synchrotron radiation. Usually, TOF mass spectra provide only the ion branching ratios for the final ionic products originating from the precursors ABC^+ and ABC^{2+} in a μs time scale, and PIPICO spectra provide only the intensity of the dissociation channels (e.g., $AB^+ + C^+$ and $A^+ + BC^+$) of ABC^{2+}. The ratio of the molecular to the dissociative processes is usually not known. To overcome this difficulty, a method to bridge the TOF and PIPICO spectra was recently developed and applied to nitric oxide [1], carbon monoxide [2], and carbonyl sulfide [3]. This method is herein applied to the molecular and dissociative single and double photoionization of carbon dioxide. Ion branching ratios and the partial cross sections for the individual ions produced from the precursors CO_2^+ and CO_2^{2+} are also separately determined, thus enabling more detailed study of the dissociation processes of the CO_2^+ and CO_2^{2+} ions.

Previous investigations of CO_2^{2+} include photon [4–7] and electron- [8–15] impact ionization mass spectrometry, Auger spectroscopy [16], single electron capture (SEC) and translational energy spectroscopy (TES) [17], double-charge-transfer spectroscopy (DCT) [7,18–20], coincidence measurements of a cation pair (PIPICO for photoionization) [7,21–23], charge-transfer and collision-induced dissociation reactions with rare gases [24], and theoretical calculations [7,23,25–27]. Although the appearance potential of CO_2^{2+} in the literature ranges from 36.2 to 38.6 eV, the closest estimation to date seems to be 37.7±0.3 eV.

II. EXPERIMENTAL PROCEDURE

The photoionization mass spectra and PIPICO spectra were measured with the use of a TOF mass spectrometer, the details of which have been described elsewhere [28,29]. A relatively high dc electric field (2250 V/cm) was applied across the ionization region and the potential of the drift tube and the ion detector was kept at −4500 V. The TOF mass spectra and the PIPICO spectra were measured at an angle of ~55° with respect to the polarization vector where the second-order Legendre polynomial is close to zero. Under these conditions, the effects of anisotropic angular distributions of fragment ions are minimized [30]. The absolute collection efficiencies of energetic fragment ions in the TOF mass spectrometer calculated with a computer program indicate that no conditions exist under which all ion pairs are collected, even if the total kinetic energy of the fragment ions is smaller than 1 eV (collection efficiency of 97%) and the efficiency for the $O^+ + CO^+$ dissociation channel with a total kinetic energy of 20 eV is 84%.

The TOF mass spectrometer was operated in two modes for the measurement of TOF mass spectra. In mode *A*, the photoelectron signal detected by the channel electron multiplier was fed into the start input of a time-

to-amplitude converter (TAC). The storage ring was operated in a multibunch mode. In this mode of operation of the TOF mass spectrometer, the relative ion yields in single and double photoionization are affected by the different kinetic energies of each photoelectron and the different number of photoelectrons in the two processes. At 60 eV, for example, the kinetic energy of photoelectrons ejected from CO_2 (forming the ground state of CO_2^+) is of the order of 46 eV, whereas that of a photoelectron (forming the ground state of CO_2^{2+}) is about 22 eV as a maximum. These more energetic photoelectrons produced by single photoionization are more easily discriminated in the TOF mass spectrometer than those produced by double photoionization. This discrimination effect results in an underestimation of the number of ions produced by single photoionization. In contrast, the different number of ejected electrons in single and double photoionization causes an overestimation of the number of ions produced in double photoionization because the probability of forming one output pulse is higher for two electrons hitting simultaneously than for one electron [3].

In mode *B*, the rf frequency (90.115 MHz) of the storage ring was used as the start signal of the TAC by reducing it to $\frac{1}{32}$ through a frequency demultiplier. The storage ring was operated in a single-bunch mode, which was essential to obtain meaningful TOF mass spectra. A typical TOF mass spectrum measured at $h\nu=80$ eV is shown in Fig. 1, which is complicated because two or three bunches pass in front of the beam line in the time range shown in the figure, and corresponding sets of the mass spectrum are recorded. In mode *B*, it is believed that the observed mass spectra are free from the discrimination effects mentioned above because the ratio of the partial cross sections Ar^{2+}/Ar^+ measured in the region from the double photoionization threshold to 100 eV was in good agreement with previous reports [31].

Monochromatic radiation was provided by a constant-deviation grazing incidence monochromator installed at the UltraViolet Synchrotron Orbital Radiation (UVSOR) facility of the Institute for Molecular Science (IMS) in Okazaki and Al (30–60 eV) and Si (62–77.5 eV) optical filters (no filter above 80 eV). The bandpass of the monochromator was about 0.4 Å with 100-μm-wide entrance and exit slits.

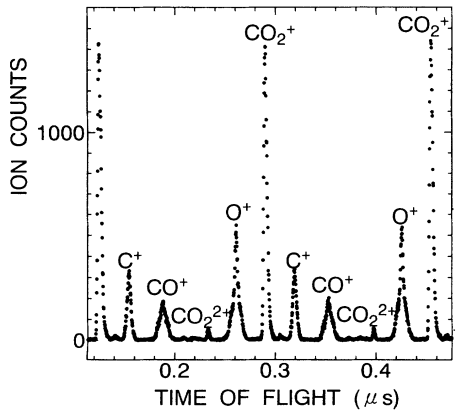

FIG. 1. Time-of-flight mass spectrum measured at a photon energy of 80 eV by using the rf frequency as the start input of a TAC (mode B). The spectrum is complicated because of the presence of two or three mass peaks, each corresponding to one particular type of ion.

III. DATA ANALYSIS

The method used for data analysis was described previously [1–3]. Because the reliable ion branching ratios for CO_2 were obtained in mode *B* in the 37–100 eV region (Sec. II), the method described for CO [2] was used. The ion branching ratios measured in the multibunch mode in the 30–36 eV range were analyzed, which are not affected by the discrimination effects mentioned above. However, the data obtained below 36.5 eV were influenced by second-order radiation because the Al filter transmits low-energy photons below 72.9 eV and were corrected in the following way. The key for the data correction is given by the ion branching ratio for CO_2^{2+}, which is not produced essentially below 36.5 eV but appears in the mass spectra due to second-order radiation. At the photon energies $E_2=h\nu\geq 36.5$ eV, where there is no second-order radiation, the apparent ion branching ratio R_A directly obtained from the TOF mass spectra is given by

$$R_A(N_j,E_2)=\frac{N_j(E_2)}{\sum_j N_j(E_2)}\ , \tag{1}$$

where N_j is the number of ions of type j. At the photon energies $E_1=h\nu\leq 36.5$ eV, where the data are influenced by second-order radiation, R_A is given by

$$R_A(N_j,E_1)=\frac{N_j(E_1)+N_j(E_2)}{\sum_j N_j(E_1)+\sum_j N_j(E_2)}\ , \tag{2}$$

where $E_2=2E_1$. For the molecular CO_2^{2+} ion, one has

$$R_A(CO_2^{2+},E_2)=\frac{N(CO_2^{2+},E_2)}{\sum_j N_j(E_2)}\equiv\alpha \tag{3}$$

and

$$R_A(CO_2^{2+},E_1)=\frac{N(CO_2^{2+},E_2)}{\sum_j N_j(E_1)+\sum_j N_j(E_2)}\equiv\beta\ , \tag{4}$$

because $N(CO_2^{2+},E_1)=0$. By solving these equations, the ion branching ratio corrected for the effects of second-order radiation, $N_j(E_1)/\sum_j N_j(E_1)$, is given by

$$\frac{N_j(E_1)}{\sum_j N_j(E_1)}=\frac{\beta}{\alpha-\beta}\left\{\frac{\alpha R_A(N_j,E_1)}{\beta}-N_j(E_2)\right\}\ , \tag{5}$$

under the condition that $\sum_j N_j(E_2)=1$. Since all quantities on the right-hand side in Eq. (5) are known, $N_j(E_1)/\sum_j N_j(E_1)$ can be obtained.

The overall scheme of photoionization and subsequent dissociation is represented by

$$CO_2+h\nu\rightarrow CO_2^+(N_s)\rightarrow C_s^+,O_s^+,CO_s^+\ (\xi_s)\ , \quad (6a)$$

$$\rightarrow CO_2^+\ (1-\xi_s)\ , \quad (6b)$$

$$\rightarrow CO_2^{2+}(N_d)\rightarrow C_d^+ + CO_d^+, C_d^+ + O_d^+ + O\ (\xi_d)\ , \quad (6c)$$

$$\rightarrow C_d^{2+}\ (\zeta_d)\ , \quad (6d)$$

$$\rightarrow CO_2^{2+}\ (1-\xi_d-\zeta_d)\ , \quad (6e)$$

where N_s and N_d represent the rates of single and double photoionization, respectively, and ξ_s and $\xi_d+\zeta_d$ are the ratios of the dissociative single and double photoionization, respectively. Although the dissociation of CO_2^{2+} into $O^+ + O^+ + C$ is possible [7], this process could not be measured by the PIPICO method with the use of a microchannel plate having a single anode. Although this dissociation channel was observed by the triple photoelectron-photoion-photoion coincidence (PEPIPICO) method [32], it is not included in the data analysis described below.

Although triple photoionization may occur above about 80 eV as observed for carbon monoxide [2], this process could not be detected by the PIPICO method because the CO_2^{3+} ions dissociate most probably into $C^+ + O^+ + O^+$. The dissociation of CO_2^{3+} into $C^{2+} + O^+$ or $C^+ + O^{2+}$ was not observed throughout the energy region studied. Since triple photoionization can be regarded as a very weak process, about one hundredth or less of double photoionization for carbon monoxide [2] and carbonyl sulfide [3], possible data contamination by this process in the evaluation of single and double photoionization is believed to be negligible.

A. Determination of single- and double-photoionization cross sections

The single- and double-photoionization cross sections σ^+ and σ^{2+} were obtained as a function of excitation energy. The ratio of double to single photoionization is given by

$$\frac{N_d}{N_s}=\frac{1}{f_i I\xi_d/C_{II}-(1+\xi_d)}\ , \quad (7)$$

where f_i is the ion-detection efficiency (ion collection efficiency in the TOF plus detection efficiency), I is the ion count rate, and C_{II} is the ion-ion coincidence rate obtained by integrating the PIPICO peaks over all ion-pair processes. The apparent ion branching ratio $R_A(CO_2^{2+}+C^{2+})$ for the doubly charged CO_2^{2+} and C^{2+} ions obtained directly from the mass spectrum is given by

$$R_A(CO_2^{2+}+C^{2+})=\frac{(1-\xi_d)N_d}{N_s+(1+\xi_d)N_d}\ . \quad (8)$$

From these equations, ξ_d, for example, is given by

$$\xi_d=\frac{x-R_A-xR_A}{(R_A+1)x}\ , \quad (9)$$

where $x=N_d/N_s$. These rates (N_s and N_d) were converted to the cross sections of single and double photoionization by using the total photoionization cross sections measured by Samson and Haddad [33].

B. Determination of the ion branching ratios and the partial cross sections for the fragmentation of CO_2^+ and CO_2^{2+}

The apparent ion branching ratio $R_A(C^+)$ for the C^+ fragment ion obtained directly from the mass spectrum at higher photon energies is the sum of the values for single (C_s^+) and double (C_d^+) photoionization. That is,

$$R_A(C^+)=R_A(C_s^+)+R_A(C_d^+)\ . \quad (10)$$

The two terms on the right-hand side in Eq. (10) are apparent ion branching ratios that are related to the inherent ion branching ratios $R(C_s^+)$ and $R(C_d^+)$ for the C_s^+ and C_d^+ ions, respectively (from the precursors CO_2^+ and CO_2^{2+}) by the following equations:

$$R_A(C_s^+)=\frac{N_s}{N_s+(1+\xi_d)N_d}R(C_s^+)\ , \quad (11)$$

$$R_A(C_d^+)=\frac{N_d}{N_s+(1+\xi_d)N_d}R(C_d^+)\ . \quad (12)$$

From the overall scheme of photoionization and dissociation (Eq. 6), $R(C_d^+)=\xi_d$. Thus $R_A(C_d^+)$ can be determined directly from Eq. (12). $R_A(C_s^+)$ is determined from Eq. (10), and by substituting the result into Eq. (11) we can finally determine $R(C_s^+)$.

IV. RESULTS AND DISCUSSION

A. Ion branching ratios

The apparent ion branching ratios directly obtained from the mass spectra measured in modes *A* and *B* are shown in Fig. 2 and are compared with those reported by Hitchcock, Brion, and Van der Wiel obtained by the dipole $(e,e+\text{ion})$ method [15].

The present results obtained in mode *A* are 33% lower for CO_2^+, 15% higher for CO^+, 29% higher for C^+, and 27% higher for O^+ at 100 eV than those measured in mode *B*. That is, a maximum error of about 30% occurs in mode *A*. However, the change in the apparent ion branching ratios measured in the two modes for the molecular CO_2^{2+} ion is drastic: the results in mode *A* are about 120% higher than those in mode *B* throughout the energy region studied. This clearly demonstrates the inadequacy of using the photoelectron signal as the start input of a TAC. The apparent ion branching ratios for the molecular CO_2^{2+} ion measured in mode *B* are in good agreement with the data reported by Hitchcock, Brion, and Van der Wiel [15] except for poor counting statistics in the latter. The data reported by Hitchcock, Brion, and Van der Wiel are 8% higher for CO_2^+, 5% lower for CO^+, 6% lower for C^+, and 10% lower for O^+ at 80 eV than the present results measured in mode *B*. That is, the discrepancies are within 10%. These small discrepancies may be caused by different sensitivities of the ion detec-

tors and the inherent characteristic of TAC, whereby the heavier ion (e.g., CO^+) produced from CO_2^{2+} is not counted if the ion-detection efficiency is high because the lighter O^+ ion produced as a pair with CO^+ stops the TAC. Since the ion-detection efficiency in the present study is of the order of a few percent, the heavier ion is detected with almost the same efficiency as the lighter ion.

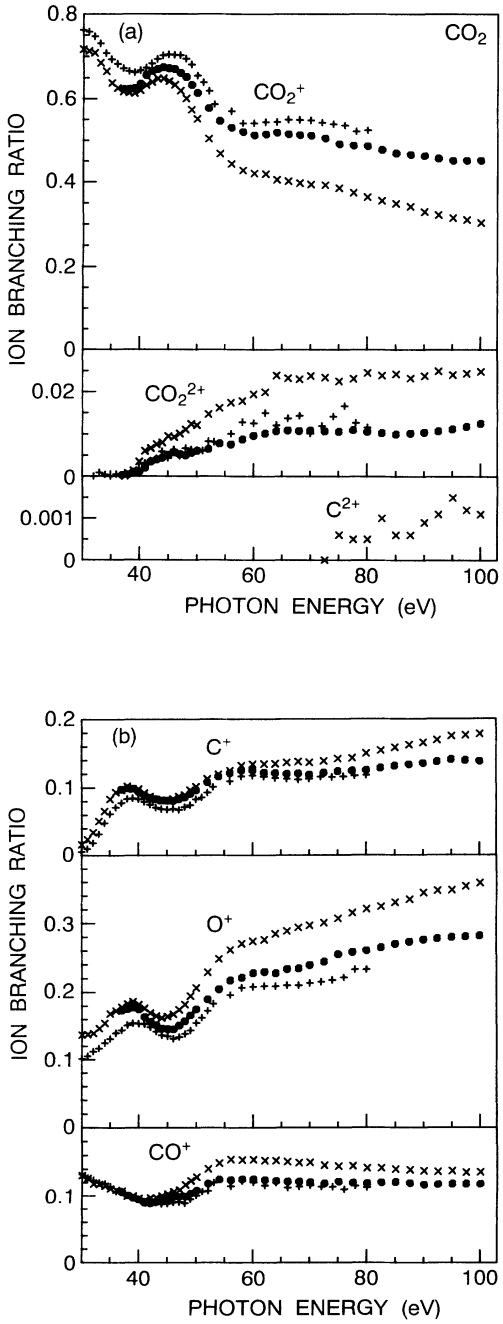

FIG. 2. Ion branching ratios directly obtained from the mass spectra as a function of photon energy. × (mode A) and ● (mode B), present data; + from Ref. [15].

B. Single- and double-photoionization cross sections

The ratio of double to single photoionization determined by the method described in Sec. III A is shown in Fig. 3 and listed in Table I. This ratio should be regarded as the lower limit of σ^{2+}/σ^+ because the $O^+ + O^+ + C$ channel of CO_2^{2+} is not included in the evaluation of σ^{2+} and discrimination effects against energetic ions produced in dissociative double photoionization have not been corrected. However, it should be noted that our σ^{2+}/σ^+ ratio for carbon monoxide [2] is in good agreement with that reported by Becker *et al.* [34] using photoelectron spectroscopy. The absolute cross sections for the single and double photoionization shown in Fig. 4 (Table I) were obtained from the total cross section σ_t [33] assuming that $\sigma_t = \sigma^+ + \sigma^{2+}$. It is emphasized that the double-photoionization cross section shown in Figs. 3 and 4 includes both the molecular and dissociative processes of the precursor CO_2^{2+}.

Dujardin and Winkoun [23] reported the value of σ^{2+}/σ_t to be 0.027 at 52 eV, which is much lower than the present data of 0.077 at the same energy. The σ^{2+}/σ_t ratios for several molecules reported by this group are systematically much lower than other literature values [1–3, and references therein].

C. Ion branching ratios and the partial cross sections for the fragmentation of CO_2^+

The ion branching ratios for the precursor CO_2^+ obtained by the method mentioned above, determined separately from those for CO_2^{2+}, are shown in Fig. 5. Three characteristic features can be seen in Fig. 5. (a) The production of the molecular CO_2^+ ion is the dominant process and its branching ratio exceeds 62% throughout the energy region examined. This trend is in accordance with NO [1] and CO [2] and in sharp contrast to OCS, for which the dissociation is dominant [3]. (b) Two shallow minima are found around 37 and 55 eV in the ion branching ratio of CO_2^+. (c) The ion branching ratios

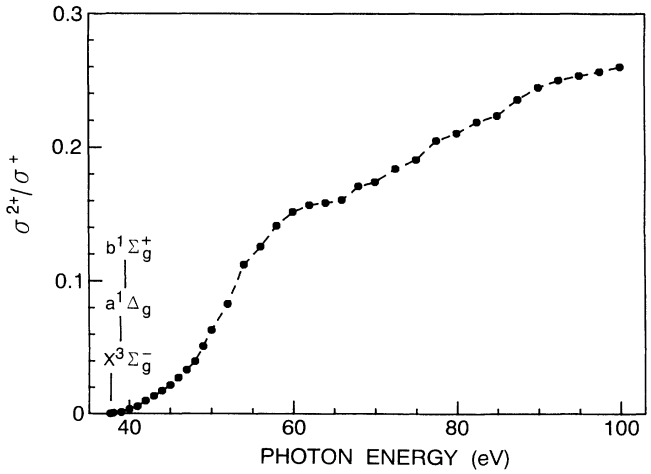

FIG. 3. Ratios of double (σ^{2+}) to single (σ^+) photoionization cross section of CO_2. The CO_2^{2+} states are from Ref. [7].

for C^+ and O^+ have a maximum around 37 eV and those for C^+ and CO^+ a maximum around 55 eV.

With respect to the dominant production of molecular CO_2^+, three routes should be considered: (a) direct single ionization with another electron excited to high-lying electronic states (CO_2^{*+}), which are bound type and stable against dissociation in a μsec time scale, (b) indirect single ionization via resonant excitation to double Rydberg states (CO_2^{**}) of the neutral, which autoionize to the high-lying bound electronic states mentioned above, and (c) double Rydberg states autoionizing to the low-lying bound electronic states, such as $X\,^2\Pi_g$, $A\,^2\Pi_u$, and $B\,^2\Sigma_u$ (Ref. [15]) of CO_2^+. The three-hole–two-particle (CO_2^{**+}) and three-hole–three-particle (CO_2^{***}) excited configurations should also be considered in these routes [7]. The last route (c) implies a two-electron transition in which one electron is removed and the other fills out a positive hole in a valence orbital like an Auger process. High-lying CO_2^{2+} states would be all dissociative because of Coulomb repulsion. Higher members of the Rydberg states converging to these CO_2^{2+} states would also be dissociative because of a simi-

TABLE I. Partial cross sections for the single and double photoionization of CO_2.

Photon energy (eV)	σ^+ (Mb)	σ^{2+} (Mb)	σ^{2+}/σ^+
30.0	27.8		
31.0	26.4		
32.0	25.8		
33.0	25.7		
34.0	25.3		
35.0	25.1		
36.0	24.8		
37.0	24.3		
38.0	24.0	0.0096	0.0004
39.0	23.0	0.025	0.0011
40.0	21.6	0.070	0.0032
41.0	20.4	0.11	0.0053
42.0	19.2	0.19	0.0097
43.0	18.1	0.24	0.013
44.0	17.1	0.29	0.017
45.0	16.4	0.36	0.022
46.0	16.1	0.44	0.027
47.0	15.7	0.52	0.033
48.0	15.1	0.60	0.040
49.0	14.7	0.75	0.051
50.0	14.6	0.92	0.063
52.0	14.2	1.18	0.083
54.0	13.3	1.49	0.112
56.0	12.6	1.58	0.126
58.0	11.7	1.66	0.141
60.0	10.8	1.63	0.152
62.0	9.86	1.54	0.157
64.0	9.24	1.46	0.158
66.0	8.51	1.36	0.160
68.0	7.93	1.35	0.171
70.0	7.41	1.29	0.174
72.5	6.99	1.28	0.184
75.0	6.47	1.23	0.191
77.5	5.89	1.21	0.205
80.0	5.53	1.17	0.211
82.5	5.19	1.14	0.219
85.0	4.91	1.10	0.223
87.5	4.57	1.07	0.235
90.0	4.28	1.04	0.244
92.5	4.05	1.01	0.250
95.0	3.85	0.97	0.253
97.5	3.64	0.93	0.256
100.0	3.43	0.89	0.260

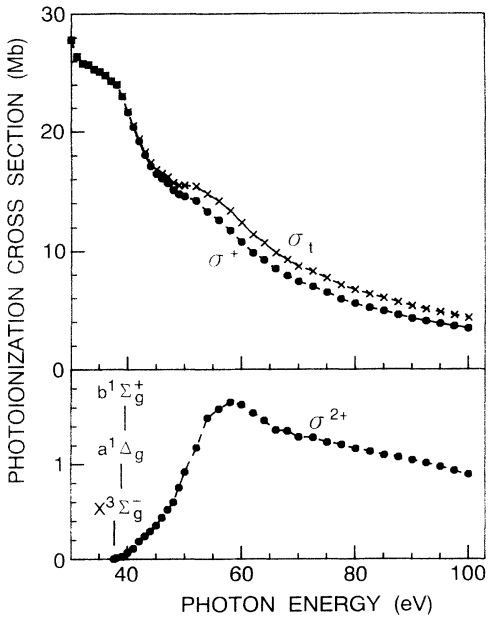

FIG. 4. Cross sections for single (σ^+) and double (σ^{2+}) photoionization of CO_2. The total cross section (σ_t) is from Ref. [33].

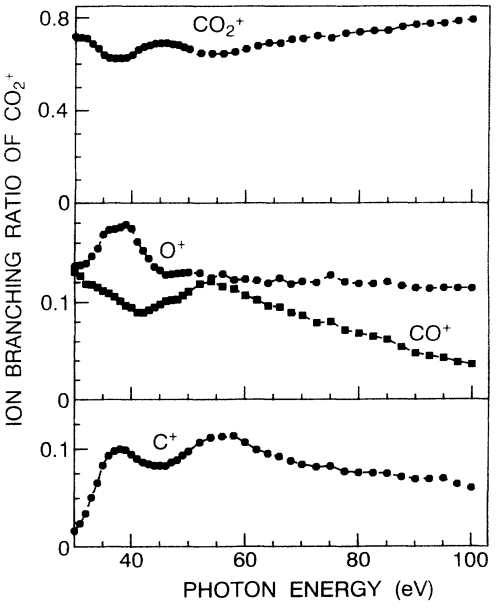

FIG. 5. Ion branching ratios of single photoionization of CO_2.

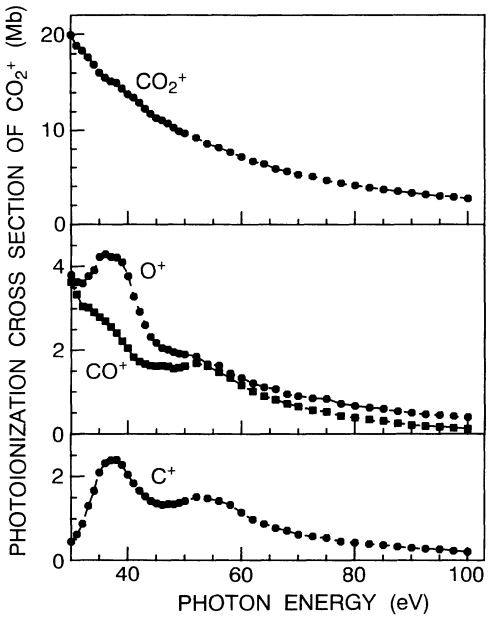

FIG. 6. Partial photoionization cross sections for the ions produced from the precursor CO_2^+.

larity of the ion core of the Rydberg states with CO_2^{2+}. If this is the case, routes (a) and (b) would not be effective and route (c) would play an important role in the production of molecular CO_2^+ at higher excitation energies.

The formation of a minimum in the ion branching ratio of CO_2^+ around 37 eV can be interpreted in the following ways. Configuration-interaction satellite bands have been observed by photoelectron spectroscopy in the 20–43 eV region [35–39]. Those bands in the 30–37 eV region would be dissociative preferably into C^+ and O^+ and those in the 37–43 eV region would be nondissociative. Above about 43 eV, the mechanisms mentioned above [(a)–(c)] open and effectively produce the stable CO_2^+ ion. The partial cross sections for the respective channels of CO_2^+ are shown in Fig. 6 (see Table II).

D. Ion branching ratios and partial cross sections for the fragmentation of CO_2^{2+}

The ion branching ratios for the precursor CO_2^{2+} separately determined from those for CO_2^+ are shown in Fig. 7. The abundance of the metastable CO_2^{2+} increases to 8.2% at 60 eV in the fragmentation of CO_2^{2+} in contrast to the value of 0.96% for the apparent ion branching ratio shown in Fig. 2, thus enabling one to evaluate the importance of the molecular CO_2^{2+} production. The $O^+ + CO^+$ and $C^+ + O^+$ ion-pair formation is dominant above 55 eV because of Coulomb repulsion between two positive holes. The partial cross sections for the respective channels are shown in Fig. 8 and listed in Table III. The appearance potential of the molecular CO_2^{2+} (37.6±0.3 eV) was found to be in excellent agreement with the value of 37.7±0.3 eV reported by Millie *et al.* [7] using photoionization mass spectrometry and further agreement with the values of 37.7±0.5 [18], 37.8±0.2 [19], 37.7±0.3 eV [20] measured by double-charge-transfer spectroscopy. The ground state of CO_2^{2+} has been assigned to be $X\,^3\Sigma_g^-$ [7]. Previously reported values for the threshold of the molecular CO_2^{2+} formation obtained by electron impact can be found in Refs. [7] and [20]. Only the metastable CO_2^{2+} ions are produced in double photoionization in the 37.6–39.2 eV region. This means that the $X\,^3\Sigma_g^-$ state is bound at least in the Franck-Condon region. The dissociation threshold of CO_2^{2+} into $O^+ + CO^+$ is found to be 39.2±0.3 eV, which is in good agreement with 39.7±0.5 eV reported by Millie *et al.* [7] and is in disagreement with 37.9±0.4 eV re-

TABLE II. Partial cross sections for the fragmentation of CO_2^+ (in Mb).

Photon energy (eV)	C^+	O^+	CO^+	CO_2^+
30.0	0.45	3.80	3.63	19.9
31.0	0.63	3.63	3.34	18.8
32.0	0.88	3.59	3.05	18.3
33.0	1.31	3.77	3.02	17.6
34.0	1.66	3.91	2.91	16.8
35.0	2.09	4.22	2.79	16.0
36.0	2.31	4.29	2.70	15.5
37.0	2.38	4.22	2.56	15.1
38.0	2.39	4.21	2.42	15.0
39.0	2.27	4.09	2.22	14.4
40.0	2.04	3.77	2.04	13.8
41.0	1.83	3.28	1.83	13.4
42.0	1.66	2.92	1.72	12.9
43.0	1.53	2.60	1.66	12.3
44.0	1.42	2.32	1.62	11.7
45.0	1.36	2.17	1.61	11.3
46.0	1.33	2.05	1.63	11.1
47.0	1.35	2.01	1.60	10.7
48.0	1.34	1.95	1.55	10.3
49.0	1.38	1.91	1.58	9.88
50.0	1.42	1.90	1.61	9.65
52.0	1.52	1.85	1.69	9.17
54.0	1.49	1.66	1.61	8.55
56.0	1.42	1.62	1.46	8.11
58.0	1.33	1.44	1.33	7.64
60.0	1.15	1.33	1.15	7.14
62.0	0.98	1.20	1.01	6.67
64.0	0.88	1.10	0.89	6.37
66.0	0.78	1.06	0.81	5.86
68.0	0.70	0.94	0.71	5.58
70.0	0.62	0.90	0.64	5.25
72.5	0.57	0.84	0.55	5.03
75.0	0.53	0.82	0.52	4.59
77.5	0.45	0.71	0.42	4.31
80.0	0.42	0.66	0.38	4.08
82.5	0.39	0.61	0.34	3.84
85.0	0.37	0.59	0.31	3.65
87.5	0.33	0.53	0.25	3.46
90.0	0.30	0.49	0.20	3.29
92.5	0.28	0.46	0.18	3.13
95.0	0.27	0.44	0.16	2.97
97.5	0.23	0.42	0.14	2.85
100.0	0.21	0.39	0.12	2.71

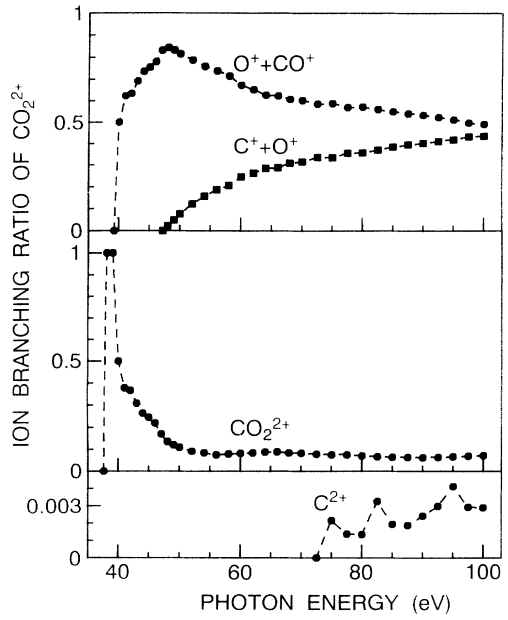

FIG. 7. Ion branching ratios of double photoionization of CO_2.

ported by Dujardin and Winkoun [23]. The dissociation of CO_2^{2+} into $C^+ + O^+ + O$ starts at 47.2±0.5 eV in close agreement with 46.4±1.5 eV reported by Millie *et al.* [7].

The low-lying electronic states of CO_2^{2+} (within a range of about 10 eV above the ground state) have been calculated by the CIPCI (configuration interaction by perturbation with multiconfigurational zeroth-order wave function selected by iterative process) method with the accuracy of the relative state energies estimated to be

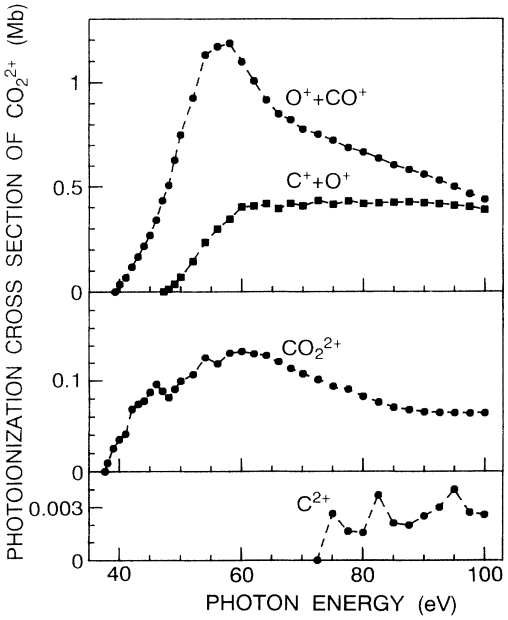

FIG. 8. Partial photoionization cross sections for the ions produced from the precursor CO_2^{2+}.

high, i.e., to within ±0.15 eV for the lower-energy states increasing to ±0.5 eV for the higher-energy states in the Franck-Condon zone [7]. Complete potential-energy surfaces are not yet available. The calculated energy states were put on an absolute scale by normalizing the calculated ground-state energy to the appearance energy (37.7 eV) of the molecular CO_2^{2+} ion. These calculated states are compared with experimental observations in Fig. 9, which shows fairly good agreement among the calculated states and the various experimental observations for singlet and triplet states. In the figure, the dissociation threshold of CO_2^{2+} into $O^+ + CO^+$ may be assigned as due to the $a\ ^1\Delta_g$ or $b\ ^1\Sigma_g^+$ state and that into $C^+ + O^+$ as due to the $^1\Delta_g$ or $^1\Sigma_g^+$ state based on energy considerations.

Above 40 eV, the ion branching ratio for the molecular CO_2^{2+} ion decreases gradually, when compared with that for NO [1], and stays almost constant above 55 eV. If there are no electronic states producing CO_2^{2+} above 55 eV, the ion branching ratio should decrease gradually. Therefore, the ion branching ratio for CO_2^{2+} above 40

TABLE III. Partial cross sections for the fragmentation of CO_2^{2+} (in kb).

Photon energy (eV)	$O^+ + CO^+$	$C^+ + O^+$	C^{2+}	CO_2^{2+}
38.0				9.6
39.0				25
40.0	35			35
41.0	68			41
42.0	118			68
43.0	166			74
44.0	216			78
45.0	268			87
46.0	341			96
47.0	432			88
48.0	506	13		81
49.0	627	37		91
50.0	749	70		100
52.0	926	145		107
54.0	1130	235		126
56.0	1170	297		119
58.0	1180	344		131
60.0	1100	402		133
62.0	1010	407		131
64.0	916	417		129
66.0	849	394		121
68.0	821	419		114
70.0	775	407		108
72.5	752	432	0.0	101
75.0	722	413	2.7	94
77.5	686	430	1.6	90
80.0	665	416	1.6	83
82.5	635	420	3.7	76
85.0	603	422	2.1	70
87.5	580	425	2.0	68
90.0	557	420	2.5	66
92.5	528	415	3.0	65
95.0	498	408	4.0	64
97.5	463	402	2.7	64
100.0	437	388	2.6	64

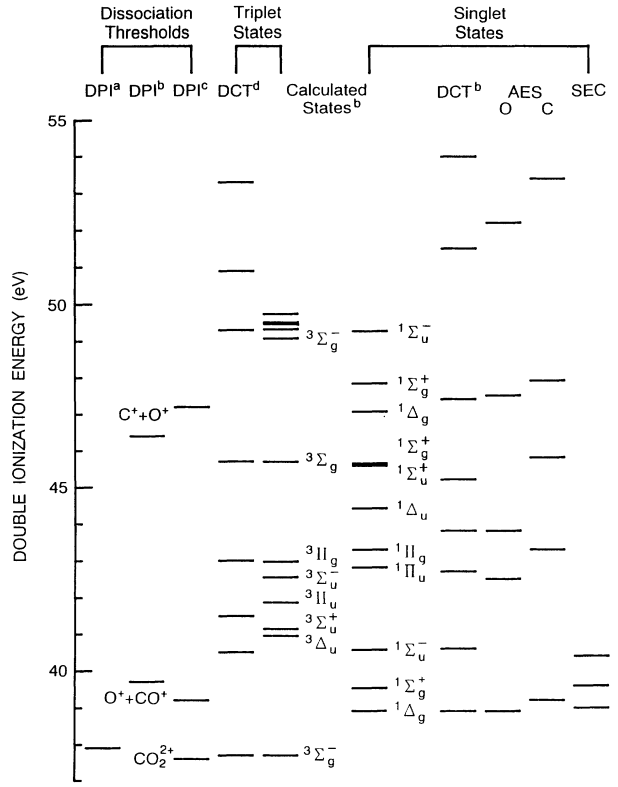

FIG. 9. Energies of singlet and triplet states of CO_2^{2+} and the dissociation thresholds of CO_2^{2+}. DPI, double photoionization; DCT, double-charge-transfer spectroscopy; AES, Auger-electron spectroscopy [16], C (carbon) and O (oxygen) peaks; SEC, single-electron capture [17]; *a*, from Ref. [23]; *b*, from Ref. [7]; *c*, present results; *d*, from Ref. [20].

eV suggests that bound or partially bound electronic states of CO_2^{2+} exist in this energy region. Another possibility for the production of metastable CO_2^{2+} is that the superexcited CO_2^{**} and CO_2^{+*} to Rydberg states converging to high-lying electronic states of CO_2^{2+} autoionize by interaction with the underlying ionization continuum of the $X\,^3\Sigma_g^-$ state.

The charge-localized dissociation of CO_2^{2+}, forming C^{2+}, becomes appreciable at higher excitation energies. The appearance potential of C^{2+} is found to be in the range 73.5–74.5 eV.

E. Dissociation ratios of CO_2^+ and CO_2^{2+}

Separate determinations of the ion branching ratios for the precursors CO_2^+ and CO_2^{2+} were used to obtain the dissociation ratios (ξ_s and $\xi_d+\zeta_d$) of the singly and doubly charged precursors, and the results are shown in Fig. 10. The dissociation ratio of CO_2^{2+} is larger than 0.90 above 50 eV. This trend is very similar to the results obtained for OCS^{2+} [3], NO^{2+} [1], and CO^{2+} [2]. Although the dissociation ratio of molecular dications has been examined for only four molecules such as OCS, NO, CO, and CO_2 so far, the high dissociation ratio of dications can be regarded as a general phenomenon even if some metastable dications are produced. This is because

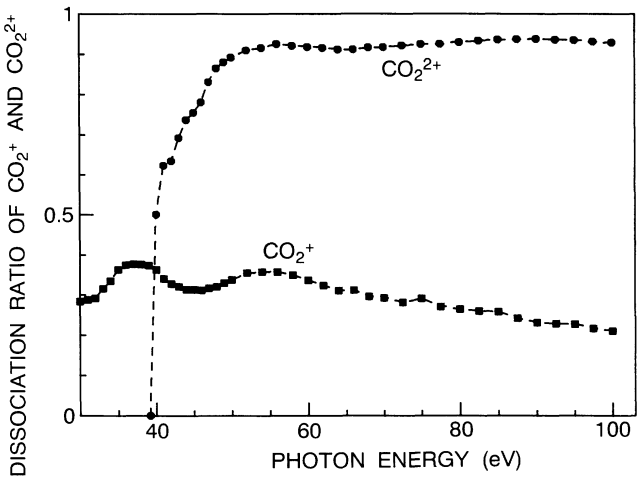

FIG. 10. Dissociation ratios of the CO_2^+ and CO_2^{2+} precursors.

only a few low-lying electronic states of molecular dications are quasibound, if any. Conversely, the dissociation ratio of molecular cations (AB^+) splits into two groups: a high dissociation ratio in the case of OCS [3] and a low dissociation ratio (say less than 40%) for NO [1], CO [2], and CO_2 below 100 eV, although details of differentiating these two groups cannot be clearly determined at present.

V. CONCLUSIONS

By developing a method to analyze mass and PIPICO spectra, the cross sections for the single and double photoionization have been determined for CO_2, in which both molecular and dissociative processes take place concomitantly. The method employed in the present study also makes it possible to determine the ion branching ratios and the partial cross sections for the ions produced from the precursor CO_2^+ separately from those of CO_2^{2+}, even at excitation energies where the molecular and dissociative single- and double-photoionization processes compete. It was found that in the single photoionization the production of the stable CO_2^+ ions is a dominant process throughout the energy region examined, whereas in the double photoionization the dissociation becomes the dominant process because of a strong Coulomb repulsion between two positive holes. For the production of the stable CO_2^+ and CO_2^{2+} ions at higher photon energies, it is pointed out that the bound-type electronic states of CO_2^+ and CO_2^{2+} do exist and/or the Rydberg states play an important role through autoionization. The charge-localized dissociation of CO_2^{2+} leading to the production of C^{2+} is also observed as a minor process in the region of the inner-valence double photoionization.

ACKNOWLEDGMENTS

Sincere gratitude is extended to the UVSOR personnel for their beneficial assistance during the experiments. This work was supported by the UVSOR Joint Research Program of the Institute for Molecular Science and in part by a Grant from Osaka City University.

[1] T. Masuoka, Phys. Rev. A **48**, 1955 (1993).
[2] T. Masuoka and E. Nakamura, Phys. Rev. A **48**, 4379 (1993).
[3] T. Masuoka and H. Doi, Phys. Rev. A **47**, 278 (1993).
[4] J. A. R. Samson, P. C. Kemeny, and G. N. Hadad, Chem. Phys. Lett. **51**, 75 (1977).
[5] B. P. Tsai and J. H. D. Eland, Int. J. Mass Spectrom. Ion Phys. **36**, 143 (1980).
[6] T. Masuoka and J. A. R. Samson, J. Chim. Phys. **77**, 623 (1980).
[7] P. Millie, I. Nenner, P. Archirel, P. Lablanquie, P. G. Fournier, and J. H. D. Eland, J. Chem. Phys. **84**, 1259 (1986).
[8] F. H. Dorman and J. D. Morrison, J. Chem. Phys. **35**, 575 (1961).
[9] A. S. Newton and A. F. Sciamanna, J. Chem. Phys. **40**, 718 (1964).
[10] K. E. McCulloh, T. E. Sharp, and H. M. Rosenstock, J. Chem. Phys. **42**, 3501 (1965).
[11] T. D. Märk and E. Hille, J. Chem. Phys. **69**, 2492 (1978).
[12] R. G. Cooks, D. T. Terwilliger, and J. H. Beynon, J. Chem. Phys. **61**, 1208 (1974).
[13] J. H. Agee, J. B. Wilcox, L. E. Abbey, and T. F. Moran, Chem. Phys. **61**, 171 (1981).
[14] B. Brehm, U. Frobe, and H. P. Neitzke, Int. J. Mass Spectrom. Ion Phys. **57**, 91 (1984).
[15] A. P. Hitchcock, C. E. Brion, and M. J. Van der Wiel, Chem. Phys. **45**, 461 (1980).
[16] W. E. Moddeman, T. A. Carlson, M. O. Krause, B. P. Pullen, W. E. Bull, and G. K. Schweitzer, J. Chem. Phys. **55**, 2317 (1971).
[17] P. Jonathan, M. Hamdan, A. G. Brenton, and G. D. Willett, Chem. Phys. **119**, 159 (1988).
[18] W. J. Griffiths and F. M. Harris, Int. J. Mass Spectrom. Ion Processes, **87**, 349 (1989).
[19] C. J. Reid, Int. J. Mass Spectrom. Ion Processes, **110**, 195 (1991).
[20] M. L. Langford, F. M. Harris, C. J. Reid, J. A. Ballantine, and D. E. Parry, Chem. Phys. **149**, 445 (1991).
[21] A. V. Shah, R. M. Wood, A. K. Edwards, M. F. Steuer, and M. N. Monce, J. Chem. Phys. **79**, 1099 (1983).
[22] D. M. Curtis and J. H. D. Eland, Int. J. Mass Spectrom. Ion Processes, **63**, 241 (1985).
[23] G. Dujardin and D. Winkoun, J. Chem. Phys. **83**, 6222 (1985).
[24] S. D. Price, S. A. Rogers, and S. R. Leone, J. Chem. Phys. **98**, 9455 (1993).
[25] J. A. Kelber, D. R. Jennison, and R. R. Rye, J. Chem. Phys. **75**, 652 (1981).
[26] H. Ågren, J. Chem. Phys. **75**, 1267 (1981).
[27] G. E. Laramore, Phys. Rev. A **29**, 23 (1984).
[28] T. Masuoka, T. Horigome, and I. Koyano, Rev. Sci. Instrum. **60**, 2179 (1989).
[29] T. Masuoka and I. Koyano, J. Chem. Phys. **95**, 909 (1991).
[30] T. Masuoka, I. Koyano, and N. Saito, Phys. Rev. A **44**, 4309 (1991).
[31] D. M. P. Holland, K. Codling, J. B. West, and G. V. Marr, J. Phys. B **12**, 2465 (1979).
[32] T. Masuoka (unpublished).
[33] J. A. R. Samson and G. N. Haddad (unpublished).
[34] U. Becker, O. Hemmers, B. Langer, A. Menzel, R. Wehlitz, and W. B. Peatman, Phys. Rev. A **45**, R1295 (1992).
[35] C. J. Allan, U. Gelius, D. A. Allison, G. Johansson, H. Siegbahn, and K. Siegbahn, J. Electron Spectrosc. Relat. Phenom. **1**, 131 (1972).
[36] C. E. Brion and K. H. Tan, Chem. Phys. **34**, 141 (1978).
[37] W. Domcke, L. S. Cederbaum, J. Schirmer, W. von Niessen, C. E. Brion, K. H. Tan, Chem. Phys. **40**, 171 (1979).
[38] P. Roy, I. Nenner, P. Millie, and P. Morin, J. Chem. Phys. **84**, 2050 (1986).
[39] H.-J. Freund, H. Kossmann, and V. Schmidt, Chem. Phys. Lett. **123**, 463 (1986).